ELSEVIER

0141-0296(95)00100-X

Engineering Structures, Vol. 18, No. 1, pp. 13–28, 1996

0141-0296/96 $15.00 + 0.00

Normalized energy-based methods to predict the seismic ductile response of SDOF structures

Michel Bruneau and Niandi Wang

Department of Civil Engineering, 161 Louis Pasteur, University of Ottawa, Ottawa, Ontario, Canada, K1N 6N5

(Received December 1993; revised version accepted June 1994)

In this paper, normalization procedures for simple rectangular pulse and sine-wave ground excitations are proposed. Normalized hysteretic energy spectra are then developed for a simple SDOF system subjected to these simple excitations, and studied to determine how the seismic inelastic cyclic response is expressed in these spectra. The influence of damping on these spectra is also investigated. It is found that the selected energy normalization methods, one using maximum ground velocity square and structural mass as a normalization basis, the other using structural yield strength and displacement, both produce useful dimensionless energy values. Then, the applicability of these simple normalization methods is studied for systems subjected to real earthquakes. Prediction of hysteretic energy using the previously derived pulse spectra is attempted statistically by considering earthquakes as a sequence of equivalent rectangular pulses. It is found that the normalized predicted hysteretic energy can be easily obtained for actual earthquake excitations by: firstly, converting these earthquakes into equivalent pulses; secondly, summing the values read for each pulse from the normalized hysteretic energy spectra constructed for simple rectangular pulse or sine wave excitations; and finally, adjusting the total values by ratio spectra or equations statistically calibrated against a number of real earthquake records. This simple and rapid procedure allows direct and reliable prediction of hysteretic energies without the need to resort to complex and time-consuming step-by-step nonlinear inelastic time-history analyses.

Keywords: earthquake engineering, prediction, inelastic response, energy method, hysteretic energy, single-degree-of-freedom, time-histories, pulse loading, sine wave loading

1. Introduction

Maximum permissible displacement or rotation ductility has traditionally been used as a criterion to establish inelastic design response spectra for the earthquake-resistant design of buildings. Unfortunately, because only a resultant maximum response parameter is taken into account, this approach lacks a quantifiable consideration of the full seismic inelastic cyclic response other than indirectly by arbitrarily set limits on the maximum ductility permissible for design. As an alternative, it has been suggested[1] that energy-based design methods can potentially alleviate the short-comings of the ductility factor method. However, much research is still needed before energy methods become an integrated part of the design process.

In a prior paper[2], some fundamental behavioural characteristics of the various terms of the energy balance equation applicable to earthquake engineering have been studied. However, in that paper, as in many others previously published on that topic, the results were not presented using a nondimensional analysis or format. While valuable observations were possible in spite of this dimensional dependency, the parameters of a forcing function or structural system are generally free to take any value, and should not

be constrained as was done earlier. Unfortunately, there is currently no consensus on how this nondimensional normalization should be accomplished. For example, in two recent publications[3,4] which attempted to quantify the contribution of hysteretic energy to structural damage, the ratio of hysteretic energy to input energy was proposed as a normalized measure of this damage. Yet, the definition of input energy adopted by these papers was totally different. Although, in both cases, the findings are very meaningful and valuable, the ambiguous definition of the seismic input energy, i.e. whether it should be defined based on earthquake record characteristics as suggested by some researchers[4], by Bertero's equation[1] as used by others[3], or by any other strategy, still needs to be clarified. For this reason, and to generalize the findings of a previous paper[2], normalization procedures are sought. This paper uses simple single-degree-of-freedom (SDOF) systems to investigate how energy demands can be effectively normalized.

Two normalization procedures for simple rectangular pulse and sine wave excitations are first developed. Since earthquakes can be thought of as a complex superposition of pulses and sine wave excitations, it is hoped that the normalized hysteretic energy spectra for individual rectangular pulses and sine wave excitations can be used to predict the energy demand of SDOF systems subjected to real earthquakes. In that direction, the feasibility of the two simple normalization methods is studied for systems subjected to real earthquakes. The prediction of hysteretic energy using the previously derived pulse spectra is attempted statistically by considering earthquakes as a sequence of equivalent rectangular pulses. Finally, the possibility of similar prediction by modelling real earthquakes as multiple sine wave patterns and series of separate half sine waves is also discussed. For brevity, the notation presented in the prior paper[2] will be used, and energy equations derived there will not be repeated.

2. Energy spectra

To facilitate the design of structures subjected to severe seismic dynamic excitations, it is desirable to develop energy spectra which indicate how the peak energy responses of SDOF systems vary with the characteristics of the structure for a particular excitation. If various peak energy responses are plotted as a function of structural period, strength ratio (η) and damping ratio, the resulting spectra could then be used to determine the energy response of a particular system to a specific type of excitation. In addition, various spectra could potentially be combined to derive a set of design energy spectra which would incorporate the uncertainties related to the nature of the excitation.

Hence, in order to reveal trends in the various energy spectra, develop a better understanding of their characteristics, and investigate how meaningful and stable normalization procedures can capture the inelastic seismic behaviour of simple SDOF structures, the study of energy spectra under simple dynamic excitation is essential before tackling the more complex seismic problem. The results of such analyses are reported in the following sections. There, input, kinetic, hysteretic and damping normalized energy spectra are constructed, using the NONSPEC computer program[5], for SDOF systems with periods ranging from 0.025 to 5.0 s, damping ratios of 0% and 2%, strength ratios, η, equal to 0.2, 0.4, 0.6, 0.8, 1.0, 1.02, 1.05, 1.1, 1.2, 1.3, 1.4, 1.6, 1.8 and 2.0, a 1 kg mass, and the same rectangular pulse excitation used previously[2]. It is noteworthy that the selected strength ratios are equivalent to those in the maximum displacement ductility spectra found in the existing literature[6]. This enables some verification of results by comparing the obtained maximum ductility demands.

3. SDOF subjected to rectangular pulse ground excitation

3.1. Preliminary concepts

Only a few nondimensional energy normalization procedures have been reported in the existing literature, and these have mostly used input energy as the normalizing parameter[3,4], with the difficulties and inconsistencies already reported above. Moreover, since Uang and Bertero[1] energy equations are used in this paper, it should be mentioned that they also proposed a first normalization method based on the idea that the input energy can be converted to an equivalent velocity by the following relationships

$$V_i = \sqrt{2E_i/M} \quad \text{or} \quad V_i = \sqrt{2E_i'/M} \tag{1}$$

for absolute and relative energy methods, respectively. Yet, in spite of this normalization, V_i and V_i' are not dimensionless and are not generalized in terms of structural strength or ground excitation parameters.

In order to have a general dimensionless energy measure recognizing ground excitation parameters, the maximum ground velocity, which is $\int_0^{t_d} \ddot{u}_g \, dt$ for the rectangular pulse excitation, is integrated into a first proposed normalization equation, expressed as

$$E^{NG} = \frac{2E}{M\left(\int_0^{t_d} \ddot{u}_g \, dt\right)^2} \tag{2}$$

where E can be any absolute or relative energy, i.e. E_i, E_i', E_k, E_k', E_s, E_h or E_d, and E^{NG} is that energy normalized by ground motion parameters corresponding to the input energy, or more exactly the kinetic energy produced by an infinitely stiff and strong structure subjected to the same ground excitation.

A second proposed normalization method is formulated to integrate the structural strength of an idealized structural force–displacement model, such as the classical bilinear force–displacement model, by the expression

$$E^{NR} = E/(R_y\Delta_y) \tag{3}$$

where E is any energy (as before), and E^{NR} is that energy normalized by the work needed to yield this SDOF system under monotonically increasing loading. However, since E_i, E_i', E_k, E_k', E_s and E_d do not have a known direct relationship with the aforementioned structural force–displacement relationship (also called hysteresis models) and $R_y\Delta_y$, it does not appear logical to use this second method to normalize energies other than E_h. That normalization method has also been used by other researchers[7].

Since the denominators in equations (2) and (3) are always constant with the energy unit of joules (J) for any given rectangular pulse and structure, both of the normalization methods would result in nondimensional energy quan-

Table 1 Normalized energies calculated for an example with $\xi = 0\%$, $t_d/T = 1.0$, $\eta = 1.0$

Energy term	Maximum energy: Non-normalized (J)	Maximum energy: Normalized E^{NG}	Maximum energy: Normalized E^{NR}
(a) For $M = 1$ kg, $\ddot{u}_g = 1$ m/s^2, $t_d = 0.5$ s			
E_i	0.2054	1.643	–
E_k	0.1720	1.376	–
E_s	0.003229	0.02583	–
E_h	0.03343	0.2674	5.279
E'_i	0.03661	0.2929	–
E'_k	0.003223	0.02578	–
(b) For $M = 100$ kg, $\ddot{u}_g = 4$ m/s^2, $t_d = 1.5$ s			
E_i	2915	1.619	–
E_k	2438	1.354	–
E_s	46.06	0.02559	–
E_h	477.0	0.2650	5.230
E'_i	523.1	0.2906	–
E'_k	45.81	0.02545	–

tities, i.e. the normalized energies would be unique and easily established values.

In order to illustrate the reliability of the above two normalization methods, a numerical example is now provided. A set of input parameters is arbitrarily selected as shown in *Table 1*. Nonlinear step-by-step dynamic time-history analyses are conducted, the resulting maximum energies are recorded and the normalized values are calculated. By applying the two proposed normalization methods, it can be seen that, for the same values of normalized excitation duration, t_d/T, strength ratio, η, and damping ratio, ξ, each energy term for which the normalization method is deemed applicable has a unique normalized value as expected. The small numerical inaccuracies as exhibited in *Table 1* and quantified in *Table 2* are negligible. They are mostly attributable to the different time steps chosen for the step-by-step analyses of structures having different periods, and minor round-off errors. Hence, the proposed normalization methods are promising, and normalized energy spectra will be constructed in Section 3.2.

3.2. *Normalized energy spectra*

In this section, 13 sets of energy spectra (as shown in *Figures 1–6*) are constructed. These figures consist of absolute and relative kinetic energy, strain energy, hysteretic energy, damping energy (when applicable) and absolute input energy spectra derived for undamped and lightly damped ($\xi = 2\%$) SDOF systems. All these energy spectra are constructed for SDOF systems subjected to a rectangular pulse ground excitation. The horizontal axis is normalized as a function of t_d/T and responses are calculated over the range from 0.1 to 20. The dimensionless t_d/T ratio captures the relative relationship between the duration of the rectangular pulse and the structural period. For example, when t_d/T is as small as 0.1, i.e. when the period of structure is 10 times greater than the pulse duration, the structure is mostly driven by the initial impulse magnitude as the system has hardly any time to deflect before the end of the pulse. On the other hand, when t_d/T is as big as 10, i.e. when the structural period is 10 times less than the pulse duration, the structure has sufficient time to reach very large deformation prior to the end of pulse. Pulses embedded with earthquake ground motion records are generally contained between these limits. Using a t_d value of 0.5 s, structural periods ranging between 0.025 and 5 s have been used to derive *Figures 1–6*, and within this range a large number of structural periods were considered in order to make each spectrum sufficiently smooth and continuous.

In all figures, ordinates are nondimensional normalized energy quantities with maximum values of 1.0, except for the absolute kinetic and input energies for reasons explained later. Results are presented in a linear-log format, with the same two exceptions where log-log scales are used for better readability. Note that for a given earthquake peak ground acceleration, a bigger dimensionless η value implies a greater structural strength.

In these spectra, each point represents the maximum energy response obtained for a given structure (i.e. for a selected η, ξ and T) and the specific rectangular pulse excitation (i.e. t_d/T and $\ddot{u}_g$). In other words, each individual value read from these spectra represents the maximum energy reached during the corresponding extended energy time history.

By comparing the energy spectra of the same type for the damped and undamped cases, and by studying individually the spectra of *Figures 1–6*, it is found that

- *Figures 1–5* for undamped and damped systems are very similar in shape, the undamped systems always having the higher energy demand. This effect of damping has already been described in the sample case studies of an earlier paper[2].
- The energy balance cannot be checked directly using only spectra. The sum of the maximum E_k, E_s, E_h and E_d will always be greater than the maximum E_i for a given structure since these maximum values generally occur at different times throughout the time histories. A simple

Table 2 Comparison of results from *Table 1*

Energy term	Normalized energy: E^{NG} From (a)	E^{NG} From (b)	E^{NG} Error (%)	E^{NR} From (a)	E^{NR} From (b)	E^{NR} Error (%)
E_i	1.643	1.619	1.5	–	–	–
E_k	1.376	1.354	1.6	–	–	–
E_s	0.02583	0.02559	0.93	–	–	–
E_h	0.2674	0.2650	0.90	5.279	5.230	0.93
E'_i	0.2929	0.2906	0.79	–	–	–
E'_k	0.02578	0.02545	1.3	–	–	–

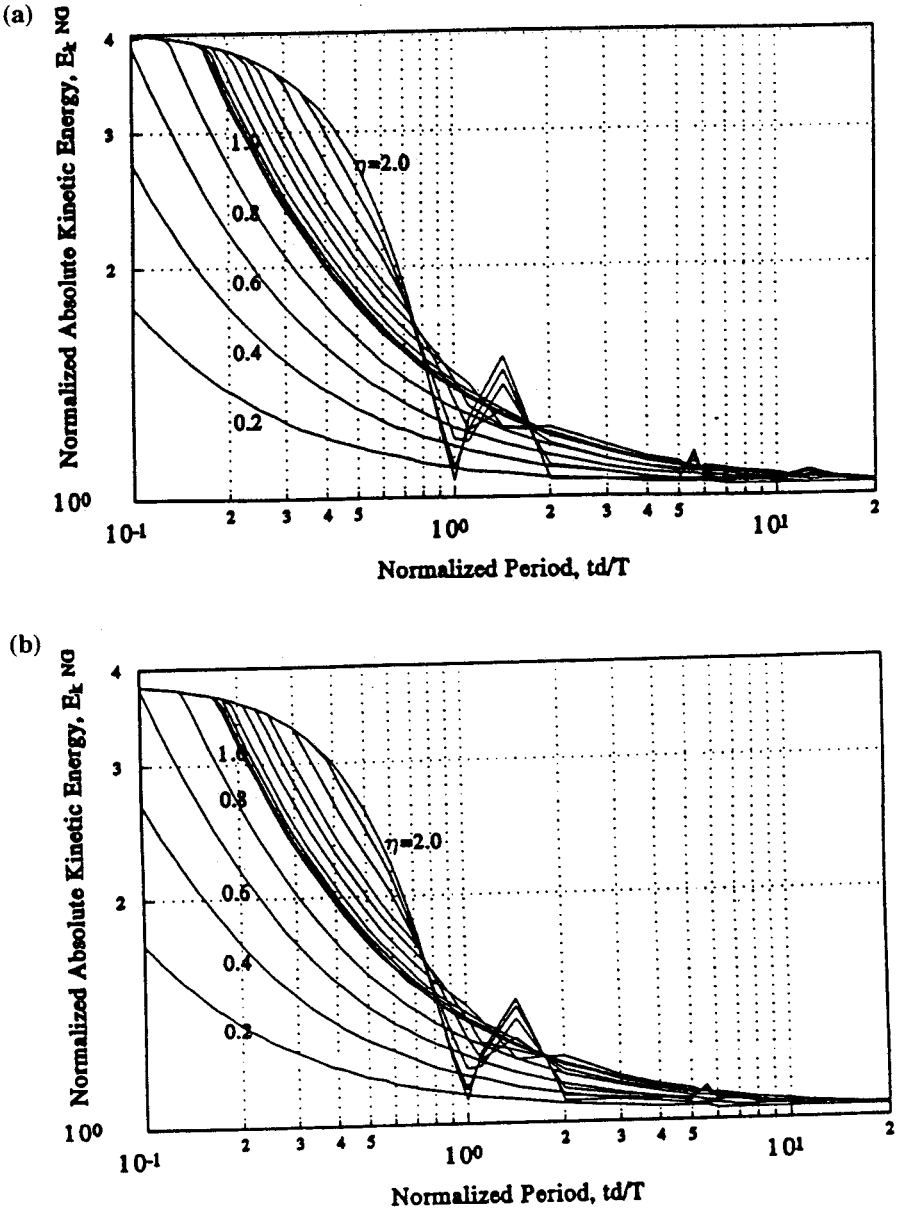

Figure 1 Normalized absolute kinetic energy spectra for rectangular pulse ground excitation: (a) undamped case ($\xi = 0\%$); (b) damped case ($\xi = 2\%$)

relationship linking the maximum energy values does not exist. However, for all cases analysed, the energy balance equation was checked to be satisfied throughout the time histories.

- The individual kinetic, strain, hysteretic and damping energies are found to be more significant and meaningful than the input energy spectra.
- The absolute kinetic energy spectra (*Figure 1*), strain energy spectra (*Figure 2*) and relative kinetic energy spectra (*Figure 5*) have similar shapes, although the absolute energy spectra always have greater values, as expected. In these spectra, the lower energies are observed to occur for the larger t_d/T and lower η values, except in the relative kinetic energy spectra where $E_k'^{NG}$ is sometimes larger for low η values, such as 0.2, 0.4, 0.6 and 0.8. This can be explained as follows, it being understood that comparing results normalized using equation (2) is conceptually equivalent to comparing systems having identical mass and ground excitation parameters (i.e. same $\ddot{u}_g$ and t_d). For a given η, a larger t_d/T results in a stiffer system. Hence, for a higher initial stiffness, displacement is less for a given force loading the structure in the elastic range; based on the definitions of the strain and kinetic energies, a smaller displacement would also cause a smaller velocity, which in turn leads to smaller strain and kinetic energies. Alternatively, from a different perspective, for a given t_d/T, a larger η value corresponds to a stronger system. Hence, for the same initial stiffness in the force–displacement relationship, R_y is larger, with potential to lead to higher strain or kinetic energy demands. This relationship between energy and period for fixed parameters of ground excitation, when t_d/T increases, could also be demonstrated analytically using the equations presented in the first paper[2] (i.e. equations 6, 8, 10, 13–15 and 17 of that paper). As for the exceptions in the relative kinetic energy spectra, which occur for structures with η of 0.2 to 0.8, in the long t_d/T range, the corresponding SDOF systems subjected to rectangular pulse excitation are so substantially under-strength, that their velocity keeps increasing

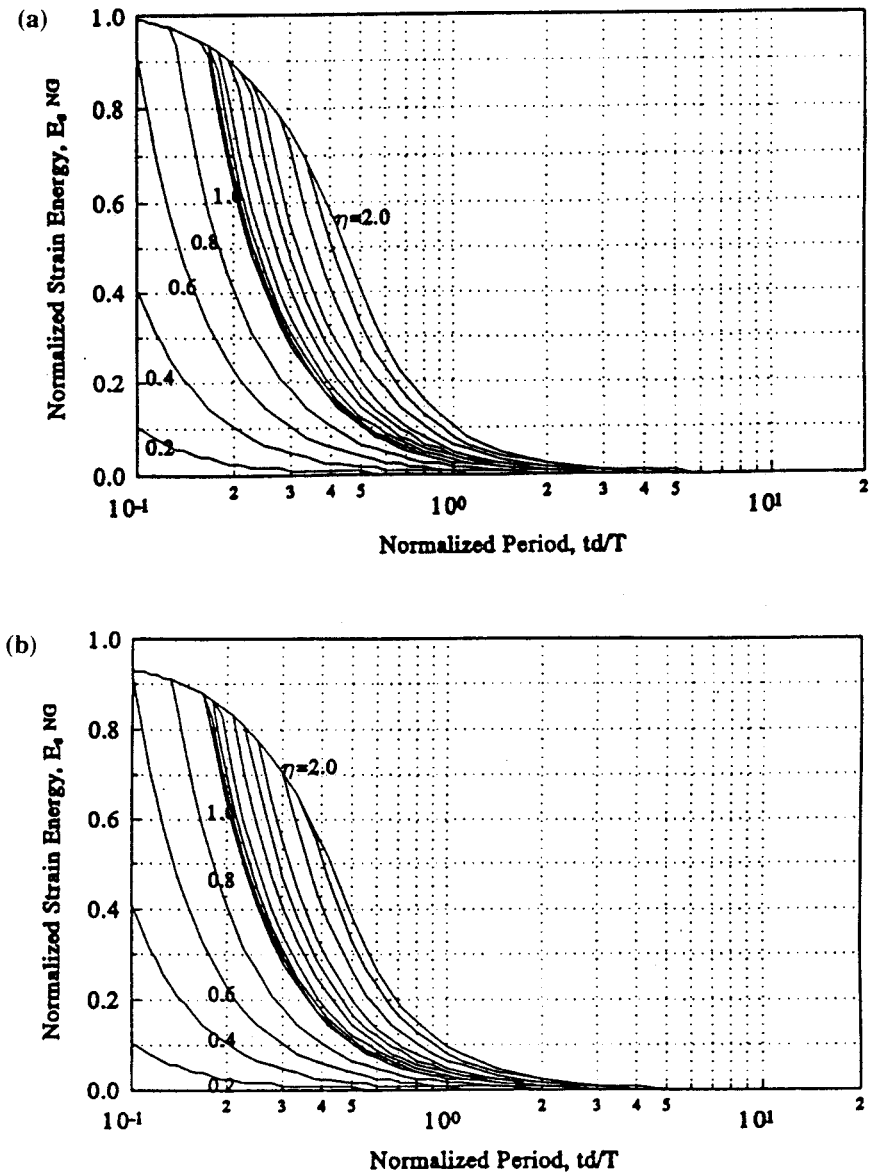

Figure 2 Normalized strain energy spectra for rectangular pulse ground excitation: (a) undamped case ($\xi = 0\%$); (b) damped case ($\xi = 2\%$)

throughout the excitation, much more rapidly than if the system remained elastic, due to the low (or zero) post-yield stiffness. Consequently, so does the maximum relative kinetic energy. However, the recoverable strain energy will not change since the yield displacement remains the same. All the energy due to displacement beyond the yield point becomes irrecoverable hysteretic energy.

- The damping and relative kinetic energies are closely related, as was demonstrated elsewhere[2]. Therefore, the total loss of relative kinetic energy due to damping becomes the maximum damping energy. This relationship also explains the peculiar shape of the damping energy spectra (*Figure 6*) in the low η and large t_d/T range (i.e. under-strength systems yielding at progressively larger velocities, as explained above for the relative kinetic energy spectra). At this point, it is worth recalling that simple viscous (velocity proportional) damping has traditionally been introduced in the dynamic equations of motion as a convenient and sufficiently accurate model for most elastic analyses even though the actual energy-loss mechanisms in real structures are likely to be more complex[8]. Thus, as a consequence of how energy methods equations are constructed, damping energy will be calculated as dissipating simultaneously to hysteretic energy when inelastic response occurs. Although this would be of significance mostly for very weak structural systems, whether this corresponds realistically to the proper physical behaviour of such structures remains to be determined.

Although not demonstrated here, it is worth mentioning that the shapes of normalized and non-normalized spectra are similar[9], which may be considered by some to be an advantage of this normalization method. Moreover, the normalization factors (i.e. the structural mass and maximum ground velocity square) can be interpreted physically as the input energy corresponding to an infinitely rigid mass resting on the ground. For that infinitely rigid mass, assuming the frictional resistance between that mass and the ground is not exceeded, the only energy that can possibly exist to balance the input energy is the kinetic energy, regardless of whether

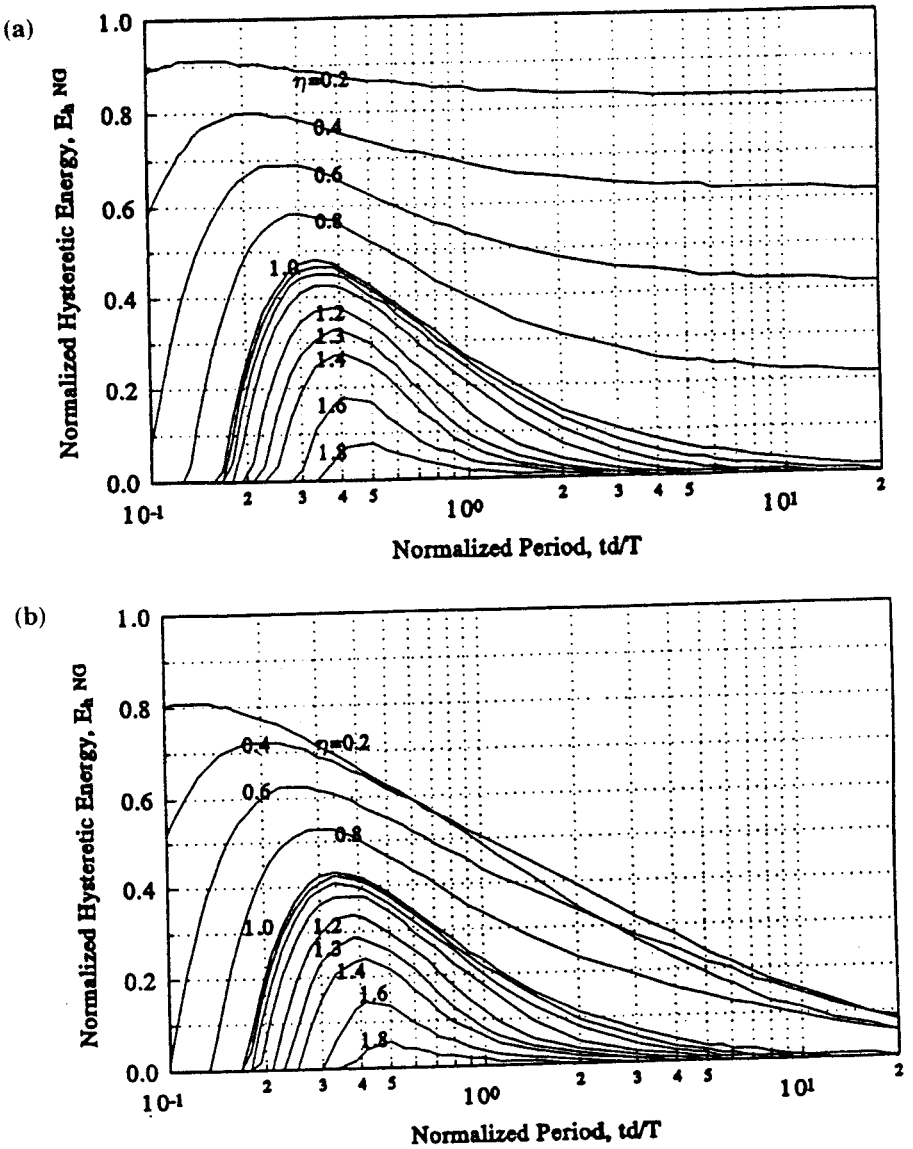

Figure 3 Normalized hysteretic energy spectra for rectangular pulse ground excitation: (a) undamped case ($\xi = 0\%$); (b) damped case ($\xi = 2\%$)

relative or absolute energy is used since relative and total velocities are identical in this case. This energy somewhat provides a measure of the raw energy potential of a given ground excitation as felt at one geographic location.

For this reason, the normalized maximum strain, hysteretic, damping or relative kinetic energy amount demanded by SDOF systems using the first method cannot exceed 1.0, since these energies are normalized by a maximum input energy. *Figures 2, 3, 5* and *6* confirm this. However, the upper bound on normalized absolute kinetic and input energies (*Figures 1* and *4*) is 4.0, which is actually reached by undamped elastic structural systems having very low t_d/T values. This result can also be easily demonstrated, using energy equations presented in the prior paper[2], classical equations of structural dynamics[8] for SDOF systems subjected to short pulse excitation, and impulse momentum relationships. For that limit case, the relative and ground motion velocities are both equal to the applied impulse divided by the mass, and added together and squared in the absolute kinetic energy equation (see definition in the earlier paper[2]); when divided by a square function of the impulse when normalized as per equation (2), all terms cancel except a constant equal to 4.0. Moreover, in undamped elastic systems, as kinetic and strain energies alternate[2], the maximum absolute input energy is identical to the absolute kinetic energy.

At the other extreme, it can be observed and rationalized that for increasingly stiff SDOF systems (i.e. with decreasing periods T, and correspondingly increasing t_d/T), the absolute kinetic and input energies (E_k^{NG} and E_i^{NG}) should converge toward a value of one, as seen in *Figures 1* and *4*, as relative velocities become progressively insignificant compared to ground velocities.

Figures 7a and *7b* are the normalized hysteretic energy spectra using the second normalization method. As mentioned earlier, this method is only logical for the hysteretic energy. Since different structures have different R_y and Δ_y values, the resultant normalized energy spectra from this method differ in shape from the non-normalized ones. Systems with smaller η and larger t_d/T have smaller R_y and Δ_y, resulting in relatively large normalized values. It can also be seen that the trends expressed in *Figures 7* and *8* can easily be understood: firstly, the structural hysteretic energy demand will increase for systems having progress-

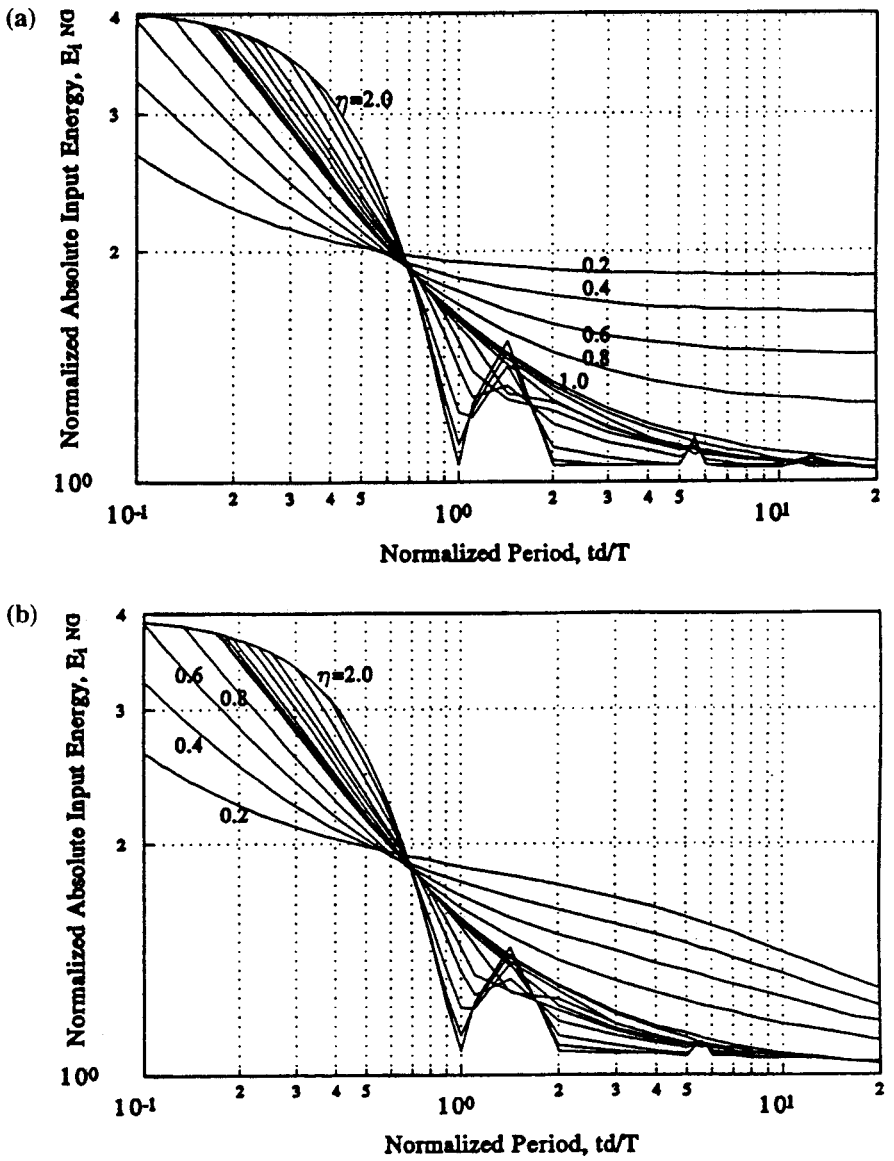

Figure 4 Normalized absolute input energy spectra for rectangular pulse ground excitation: (a) undamped case ($\xi = 0\%$); (b) damped case ($\xi = 2\%$)

ively lower η value (i.e. lower normalized strength ratio) for a given value of normalized period; secondly, for a given η, systems with shorter periods will have higher normalized hysteretic energy demand because of their correspondingly smaller yield displacements, and; finally, when η equals 2.0, E_h^{NR} will always be 0, as expected for a pulse ground excitation.

4. SDOF subjected to sine-wave ground excitation

4.1. *Preliminary concept*

As per the same logic described above for rectangular pulse excitations, normalized spectra are also needed for sine-wave ground excitations. The two normalization methods previously proposed and used are retained here. However, before constructing the normalized spectra, it must be ensured that these normalization procedures still work well for the case at hand, i.e. that the normalized spectra are generally applicable irrespectively of which parameter(s) change(s).

For the first normalization method (equation (2)), the consideration of structural mass in the method is not affected by the sine wave nature of the ground motion, but the definition of maximum ground velocity used for rectangular pulse excitation is inadequate for sine wave loading and needs to be improved. By substituting the appropriate maximum sine-wave velocity of $\ddot{u}_{gmax}\bar{T}/2\pi$ into equation (2), a first normalization method for harmonic sine-wave excitation could be proposed as

$$E^{NG} = \frac{2E}{M\left(\frac{\ddot{u}_{gmax}\bar{T}}{2\pi}\right)^2} \tag{4}$$

but since the input and the hysteretic energies are cumulative and increasing at each yield excursion[2], equation (4) is not adequate either, except for kinetic and strain energies.

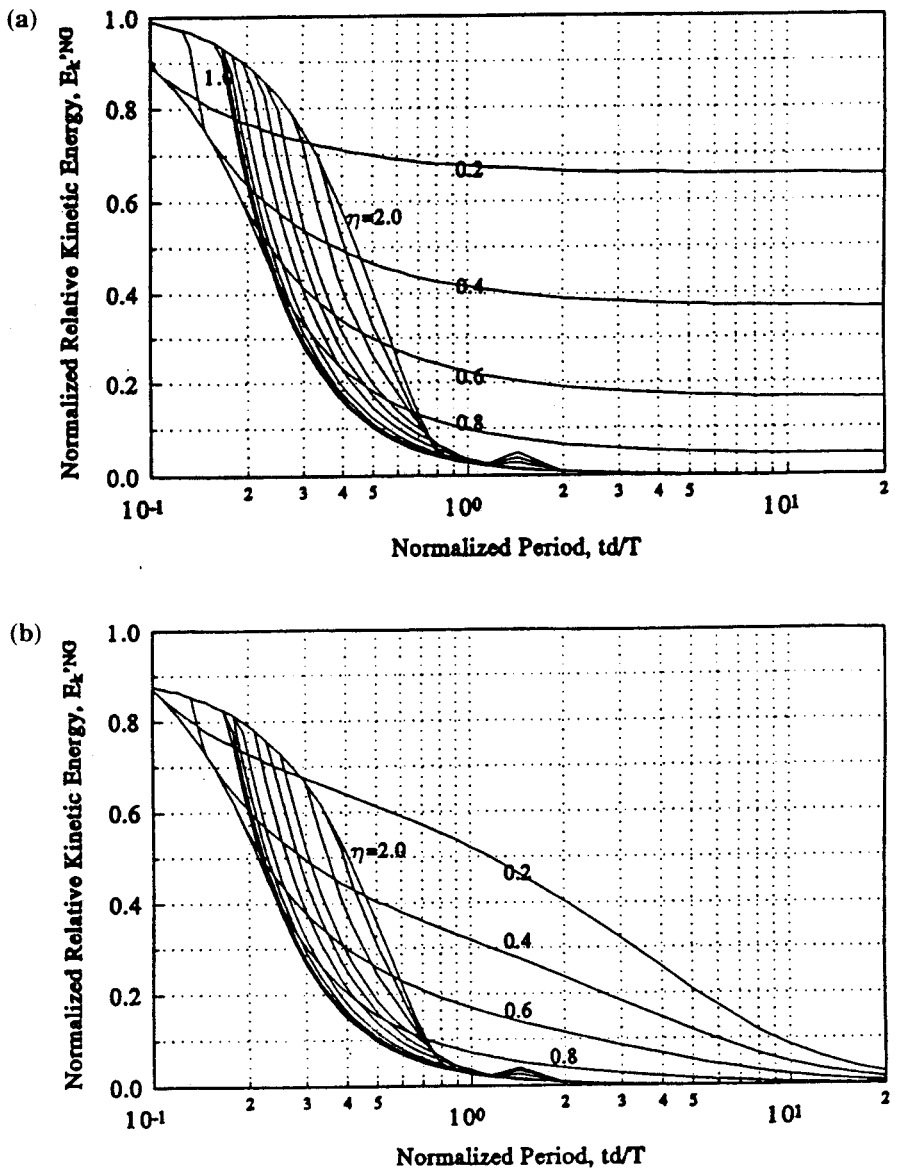

Figure 5 Normalized relative kinetic energy spectra for rectangular pulse ground excitation: (a) undamped case ($\xi = 0\%$); (b) damped case ($\xi = 2\%$)

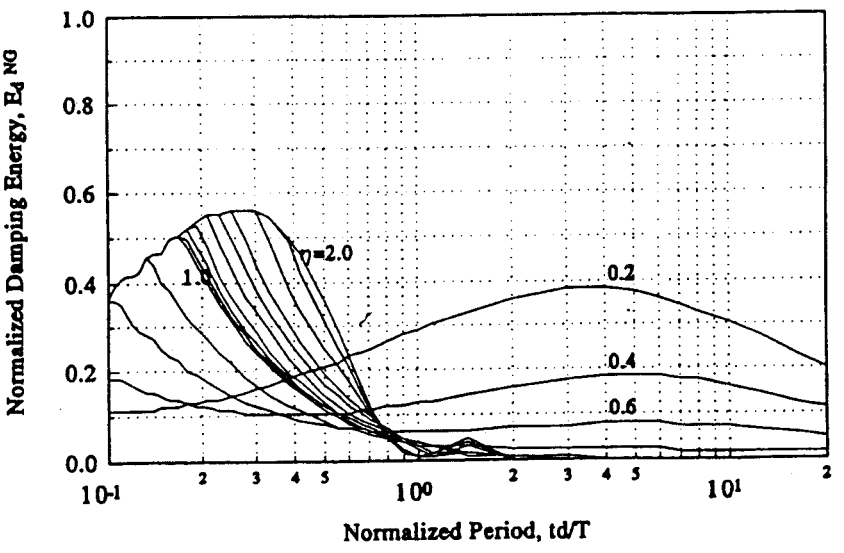

Figure 6 Normalized damping energy spectra for rectangular pulse ground excitation ($\xi = 2\%$)

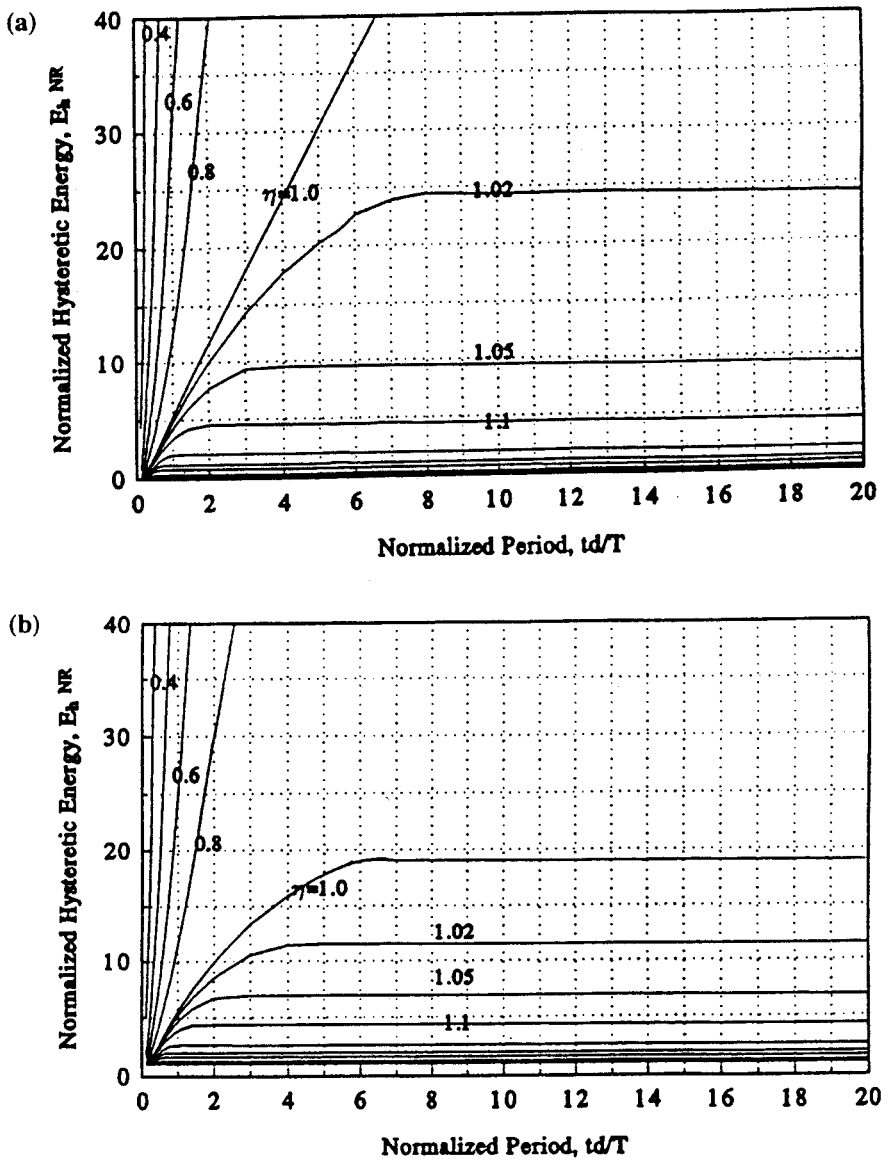

Figure 7 Normalized hysteretic energy spectra for rectangular pulse ground excitation: (a) undamped case ($\xi = 0\%$); (b) damped case ($\xi = 2\%$)

To normalize cumulative unbounded and periodic energies here, the number of cycles of the sine wave loading must be taken into account. Thus, a normalized energy per input cycle is proposed as

$$E^{NG} = \frac{2E}{NM\left(\frac{\ddot{u}_{gmax}\bar{T}}{2\pi}\right)^2} \tag{5}$$

where N is the number of cycles of a sine wave.

By the same logic, the form of the second proposed normalization method becomes

$$E_h^{NR} = E_h/(NR_y\Delta_y) \tag{6}$$

Beyond this periodicity consideration, the normalization parameters are unchanged and their rationalization need not be repeated here. However, to construct the normalized energy spectra, the dimensionless quantity, β, (defined as equal to the ratio of the natural to the applied load vibration periods, $T/\bar{T}$) is a more meaningful representation of normalized period for abscissa, and is used here.

In order to illustrate the reliability of the above proposed normalization formulae, a numerical example is provided. For a set of input parameters, arbitrarily selected and displayed in *Table 3*, the resultant maximum energies and normalized values are calculated and tabulated there. By comparing E^{NG} or E^{NR} of the two cases, it can be seen that, for the same normalized excitation period, β, strength ratio, η, and damping ratio, ξ, each energy term for which the normalization method is deemed applicable has a unique normalized value as expected. Small numerical errors as exhibited in *Table 4* are negligible for the reasons discussed earlier. Hence the proposed normalization procedures are effective, and the corresponding normalized energy spectra will be constructed in Section 4.2.

4.2. *Normalized hysteretic energy spectra*

General hysteretic energy spectra are constructed for sine wave excitations using the two proposed normalization methods. It is hoped these spectra, together with the normalized hysteretic energy spectra for rectangular pulse excitation, will be useful to predict the hysteretic energy

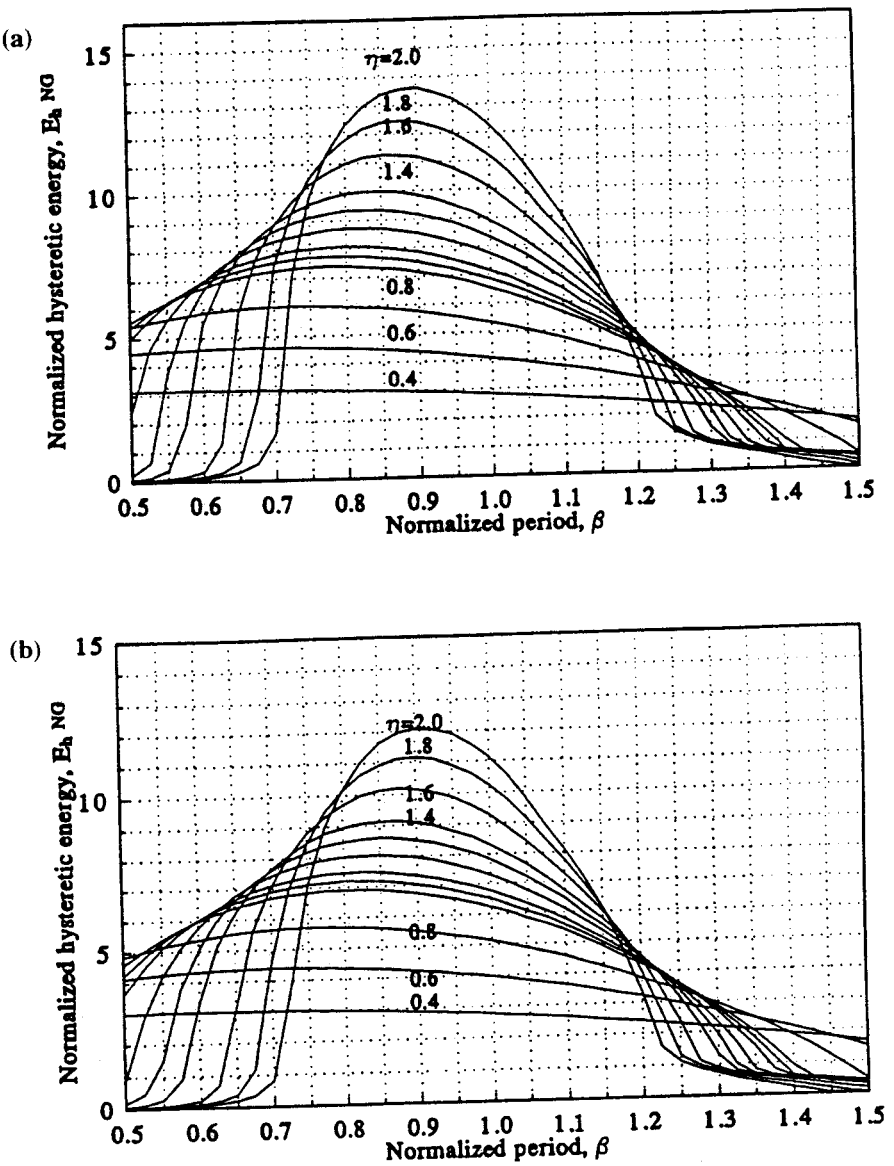

Figure 8 Normalized hysteretic energy spectra for sine-wave ground excitation: (a) undamped case ($\xi = 0\%$); (b) damped case ($\xi = 2\%$)

demand of simple systems subjected to real earthquake excitations.

Although it is possible to construct spectra for all the energy terms, as in Section 4.1, it is neither desirable nor practical to do so. The meaning and significance of each energy term has already been established above and elsewhere[2]. Kinetic and strain energies are not dissipative and are not useful in damage predictions. Moreover, while damping energy is dissipative, the hysteretic energy spectra constructed for various damping ratios indirectly accounts for the presence of this damping. Thus, the availability of hysteretic energy spectra (derived for given damping ratios) is apparently sufficient for damage predictions, and the rest of this paper will accordingly concentrate on hysteretic energy.

4.2.1. Normalization method 1

Figures 8a and *8b* are the resulting normalized hysteretic energy spectra produced using

$$E_h^{NG} = \frac{2E_h}{NM\left(\frac{\ddot{u}_{gmax}\bar{T}}{2\pi}\right)^2} \qquad (7)$$

for damping ratios of 0% and 2%, respectively. Again, using this method, the shape of the figures closely corresponds to the non-normalized hysteretic energy spectra (not presented here), as the denominator of equation (7) is constant for a given input. It is observed that the undamped normalized hysteretic energies are slightly bigger than those for systems with a 2% damping ratio.

Again, any point on a spectra corresponds to the maximum value obtained throughout a hysteretic energy time history, which itself is related to a particular physical displacement time history. This perspective helps explain why in both *Figures 8a* and *8b*, for big η values, E_h^{NG} varies much as a function of β, while for small η, it does not. In other words, for a structure nearing resonant response, if the potential to develop a strong elastic response exists prior to yielding, the structure can be visualized as entering the inelastic range with a larger velocity (i.e. a larger kinetic energy) at each cycle, which in turn requires more hysteretic energy to be stopped. Stronger structures (large η) possess more of such an elastic displacement response, whereas it can hardly develop in weak systems (small η).

Table 3 Normalized energies calculated as an example with $\xi = 0\%$, $\beta = 0.75$, $\eta = 2.0$

Energy term	Maximum energy: Non-normalized (J)	Normalized: E^{NG}	Normalized: E^{NR}
(a) For $M = 1$ kg, $\ddot{u}_{gmax} = 1$ m/s², $T = 1.5$ s, $\bar{T} = 2.0$ s, $t_d = 20$ s			
E_i	5.304	10.47	–
E_k	0.6061	11.96	–
E_s	0.1162	2.294	–
E_h	4.958	9.787	2.175
E'_i	5.086	10.04	–
E'_k	0.1836	3.624	–
(b) For $M = 100$ kg, $\ddot{u}_{gmax} = 5$ m/s², $T = 0.45$ s, $\bar{T} = 0.6$ s, $t_d = 9$ s			
E_i	1811	10.59	–
E_k	136.5	11.98	–
E_s	26.12	2.292	–
E_h	1731	10.12	2.250
E'_i	1762	10.31	–
E'_k	41.58	3.648	–

E_i, E'_i and E_h must consider the number of cycles of sine wave loading in their normalization

4.2.2. *Normalization method 2*

Figures 9a and *9b* are the normalized hysteretic energy spectra produced using

$$E_h^{NR} = E_h/(NR_y\Delta_y) \tag{8}$$

for damping ratios of 0% and 2%, respectively. Since this normalization method is related to the yield strength and displacement of the system, it is felt that these normalized spectra can reflect the structural energy demand in a more straightforward and rational manner. As revealed by both figures, systems with higher η value have lower hysteretic energy demands, i.e. stronger structures yield less and consequently have a higher ability to resist cyclic dynamic excitations.

When $\beta < 0.8$, systems start to respond as if subjected to pulse excitations, since the period of the sine wave is becoming relatively larger than the structural period and each cycle of loading could be considered as a pulse impacting the system. Thus for one cycle of excitation and a given η value, smaller β results in greater energy demand. This conversion to pulse-driven response can be further emphasized by replotting *Figure 9a* using instead ηE_h^{NG} as a new normalized energy expression in the ordinate, and superposing on these results (over the range $\beta < 0.8$) the corresponding values obtained for a double rectangular pulse and one full sine pulse ground excitation, as shown in *Figure 10*. Results between the pulses and continuous sine-wave ground excitations obviously cannot be identical, due to different initial displacement and velocity conditions at the start of each load reversal, but they confirm the rationale for the observed trend in behaviour at low β. It is also noteworthy that for $\beta > 0.8$, energy results normalized as per ηE_h^{NG} for SDOF subjected to continuous sine-wave ground excitation become superposed and vary almost linearly as a function of β.

5. SDOF systems subjected to real earthquakes

The previous sections have quantitatively expressed, through spectra, how hysteretic energy can be a good indicator of the structural nonlinear cyclic cumulative behaviour of SDOF systems subjected to simple pulse and sine wave ground excitations. It remains to investigate how these spectra can be used to predict hysteretic energy demand under real earthquake excitation. Five major earthquakes will be considered to obtain the statistical information needed for reliable prediction spectra. They are the Imperial Valley El Centro Earthquake of 18 May 1940 (S00E component), San Fernando Pacoima Dam Earthquake of 9 February 1971 (S16E component), Helena Montana Earthquake of 31 October 1935 (S00W component), Western Washington Olympia Earthquake of 13 April 1949 (N04W component), and the Parkfield California Earthquake of 27 June 1966 (N65E component).

5.1. *Extension of proposed normalization methods to real earthquakes*

Two normalization methods have been proposed in Sections 3 and 4. The first one uses the maximum ground velocity and structural mass in its normalization equation, whereas the second one considers structural yield strength and displacement. Both performed very well for the simple rectangular pulse and sine wave excitations. For real earthquake excitations, it is difficult to directly normalize the hysteretic energy against a unique value of maximum ground velocity as per the first method; the highly random nature of any given earthquake excitation makes compliance to such a rigid framework difficult. A number of different normalization approaches built from extensions or modification of this first normalization method have been considered, with the constraint that the normalizing parameter had to be an expression of energy, but none proved to be dominantly superior to the one adopted in the remainder of this work.

Table 4 Comparison of results from *Table 3*

Energy term	Normalized energy: E^{NG} From (a)	E^{NG} From (b)	E^{NG} Error (%)	E^{NR} From (a)	E^{NR} From (b)	E^{NR} Error (%)
E_i	10.59	10.47	1.1	–	–	–
E_k	11.98	11.96	0.17	–	–	–
E_s	2.292	2.294	0.087	–	–	–
E_h	10.21	9.787	3.2	2.175	2.250	3.4
E'_i	10.31	10.04	2.6	–	–	–
E'_k	3.624	3.648	0.66	–	–	–

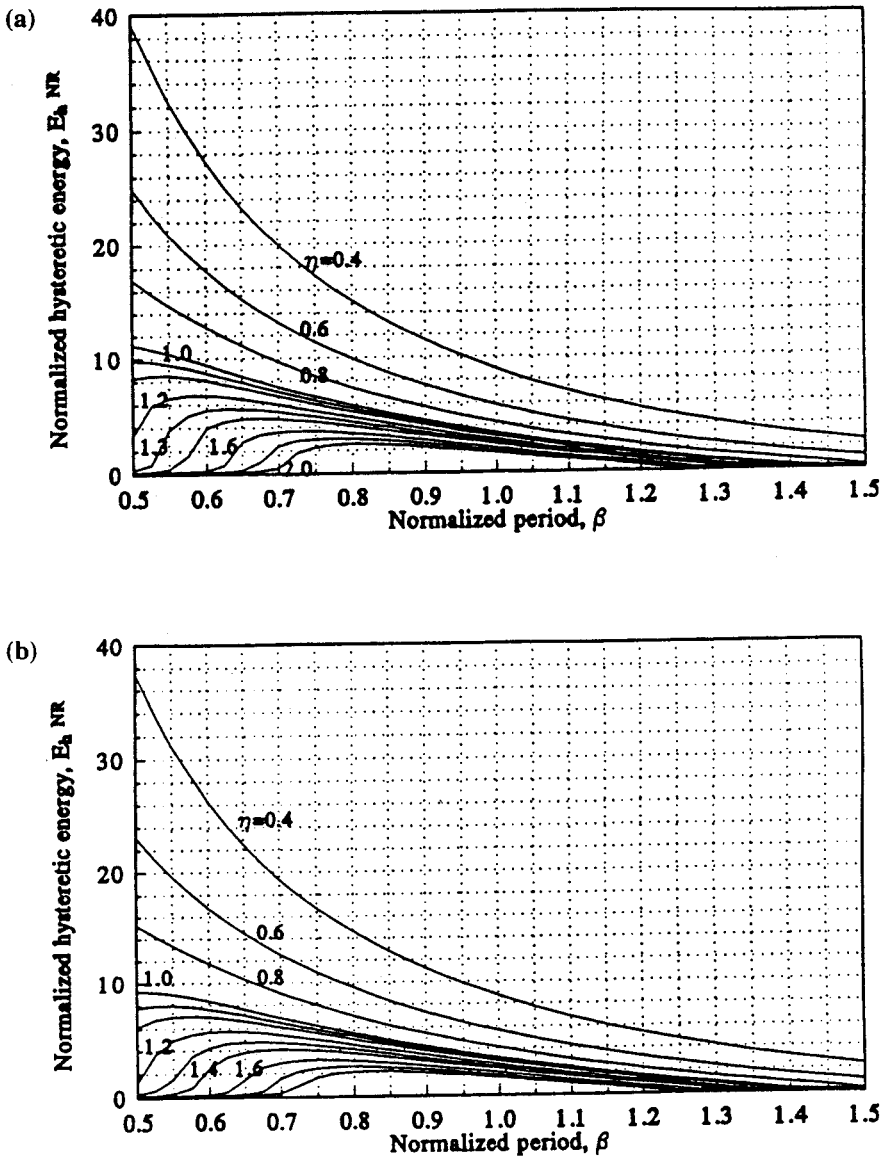

Figure 9 Normalized hysteretic energy spectra for sine-wave ground excitation: (a) undamped case ($\xi = 0\%$); (b) damped case ($\xi = 2\%$)

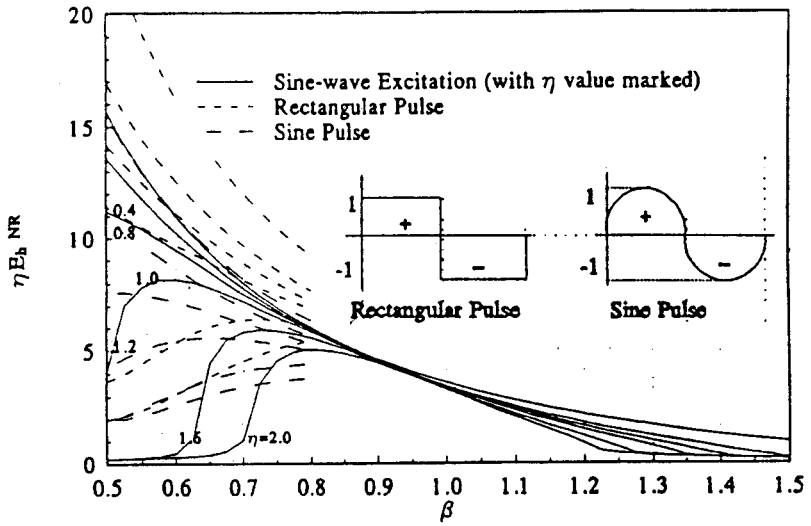

Figure 10 Comparison of normalized hysteretic energy spectra under sine-wave ground excitation, and double rectangular and sine pulse ground excitations

Contrary to the above, the second proposed normalization method is easily applicable with real earthquake excitations, as the yield strength, R_y, and yield displacement, Δ_y of any structure is independent of the nature of ground excitation. However, it is used only with the hysteretic energy spectra for the reasons mentioned earlier. Hence, only this second normalization method is used thereafter.

For use in a design procedure, normalized hysteretic energy spectra could obviously be directly constructed for a group of earthquakes. This operation is computer intensive, but rational and theoretically correct. However, it would be advantageous if hysteretic energy could be directly predicted from spectra derived from simpler forms of ground excitation. This is investigated below.

5.2. *Prediction of seismic hysteretic energy by equivalent rectangular pulses method*

In this section, a procedure is developed to predict seismic hysteretic energy from spectra derived for rectangular pulse excitations. For this purpose, any earthquake must first be modelled as a sequence of rectangular pulses. For a given earthquake's ground acceleration time history record, each of the numerous crossings of the zero axis delimitates the boundaries of a positive or negative area. Any such single positive or negative area can be considered as a pulse with a maximum acceleration value and a corresponding area. In order to change such an irregularly shaped pulse to an equivalent rectangular pulse of the same maximum acceleration and area, an equivalent time duration, t_d, must be defined. By repeating the same procedure to every area thus defined by two consecutive crossings of the time axis of the earthquake acceleration time history diagram, an actual earthquake record can be replaced by a sequence of discontinuous rectangular pulses. The resulting distribution of such equivalent pulses for a particular earthquake is shown in *Figure 11*.

Computer programs were written to make the above procedure simple, fast and more accurate[9]. One simple program converts the raw earthquake acceleration data into a sequence of equivalent rectangular pulses defined by their amplitudes and equivalent durations, and a second program calculates the cumulative normalized hysteretic energy. Due to their extreme simplicity, both programs can be executed in a few seconds. For the later program, information on the previously constructed normalized hysteretic energy spectra for rectangular pulse excitation is contained in a matrix, and the corresponding hysteretic energy for a given equivalent pulse can be directly obtained by double interpolation. The resulting sum of these portions of normalized hysteretic energies calculated by the computer program is actually a raw predicted normalized hysteretic energy for a given earthquake, and noted as $E_h^{NR'}$. This $E_h^{NR'}$ is then compared with the true normalized hysteretic energy noted as E_h^{NR} directly and separately calculated for the earthquake itself using NONSPEC. Finally, the ratio of predicted to actual hysteretic energy can be determined for an ensemble of earthquakes.

Statistical results are generated for the five selected earthquakes. For each earthquake, the true normalized hysteretic energies, E_h^{NR}, and corresponding predicted values, $E_h^{NR'}$, are calculated and compared for various undamped SDOF systems over ten structural periods (0.1 s, 0.2 s, 0.3 s, 0.4 s, 0.6 s, 0.8 s, 1.0 s, 1.25 s, 1.5 s and 2.0 s) and six structural strength ratios (0.4, 0.6, 0.8, 1.0, 1.2 and 1.4). Here, only the 0% damping ratio case is considered, the principle would be the same for damped systems.

However, the obtained predicted results are often not close to the actual earthquake ones. This discrepancy is understandable because the equivalent rectangular pulse method assumes a zero initial velocity and displacement at the beginning of every pulse, which is not the case during a real earthquake excitation. Nonetheless, a certain trend was discovered to exist for the ratio of $E_h^{NR'}$ to E_h^{NR} as a function of different structural periods and strength ratios.

The simplest way to establish the relationship between the predicted and actual normalized hysteretic energy results is to construct their ratio spectra. To immediately establish the general trend for an average of many earthquakes, instead of building one set of spectra for each earthquake, the mean curves for five earthquakes are constructed as a function of various structural periods and strength ratios, as shown in *Figure 12a*. For completeness, the mean plus one standard deviation curves are also constructed in *Figure 12b*. It is noteworthy that the mean minus one standard deviation curves could be just as easily derived. It can be observed from *Figure 12* that in most circumstances

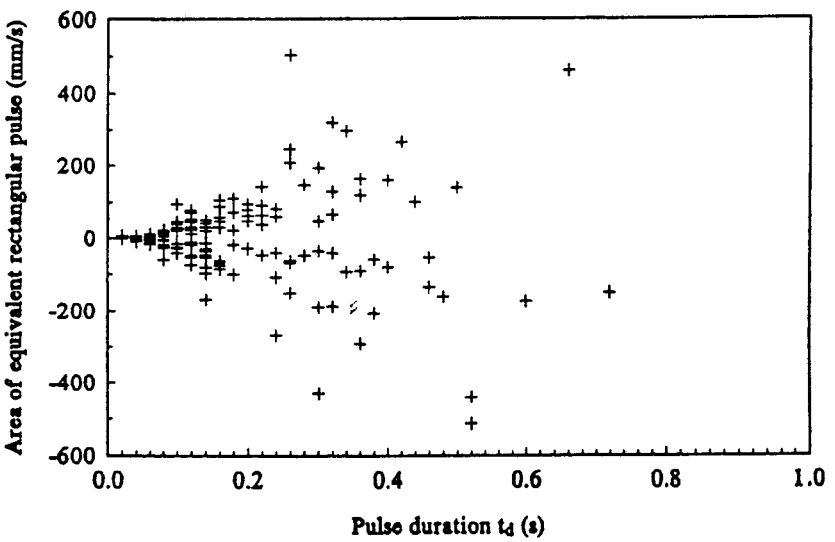

Figure 11 Distribution of equivalent pulses of El Centro earthquake

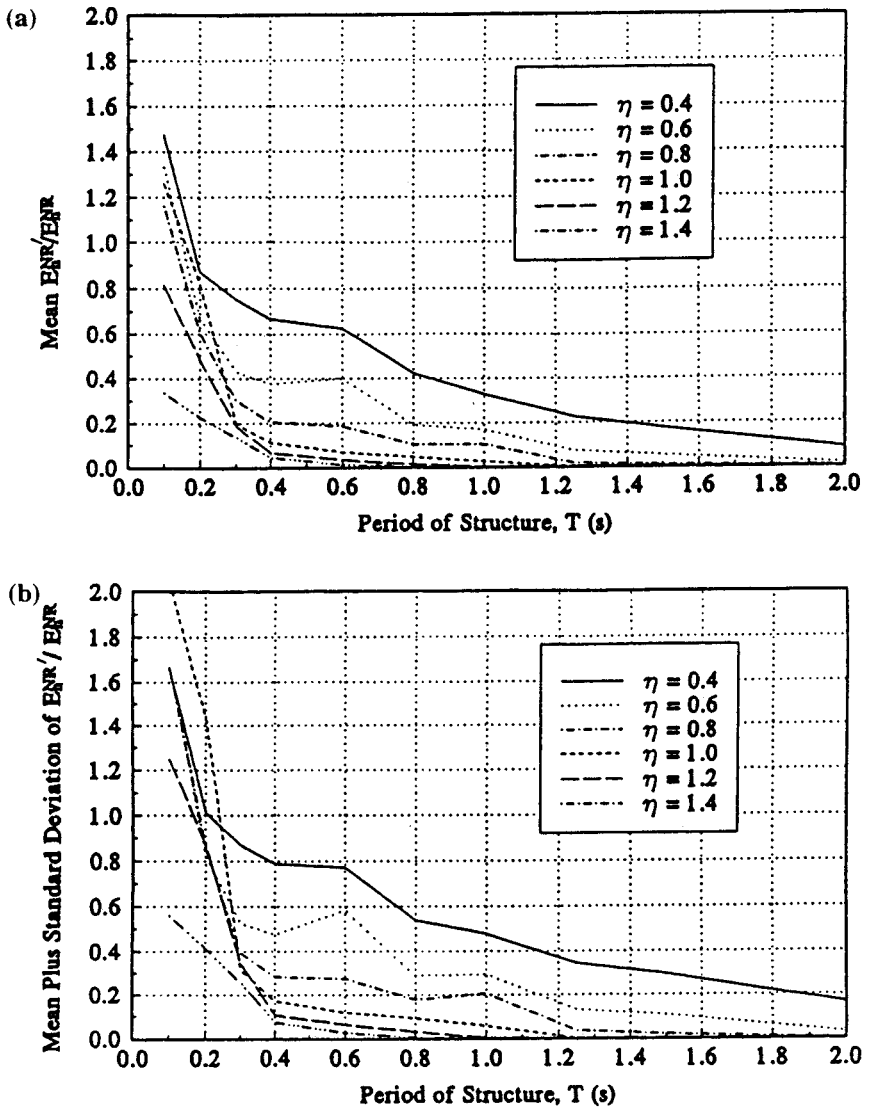

Figure 12 (a) Mean ratio-spectra based on five earthquakes converted to rectangular pulses: (b) mean plus one standard deviation ratio spectra

except for systems with very short periods and low η values, the ratio of $E_h^{NR'}/E_h^{NR}$ is less than 1, which implies that the predicted results 'under-predict' the normalized hysteretic energy demand. Therefore, an effective prediction method must take into account and correct this deficiency.

Assuming that the five earthquake records used to derive *Figure 12* are representative earthquakes for selected regions of the world, empirical equations for the $E_h^{NR'}/E_h^{NR}$ ratio can be derived to allow direct and accurate prediction of hysteretic energy. Using exponential curves, which appear to adequately represent the trends in data, best curve fitting is done based on linear regression analysis. The resulting equations for the six strength ratios are derived in *Table 5*. The accuracy of the resulting curve fitting for *Figure 12* is quite acceptable, as illustrated in *Figure 13* for an arbitrarily selected parameter-set. Interpolation between the curves for various η can also be performed if necessary.

To more explicitly demonstrate how the aforementioned procedure works to predict the hysteretic energy demand for a specific SDOF system, the whole procedure is reviewed for a SDOF system with period of 0.4 s and strength ratio of 0.6 subjected to the El Centro earthquake. Using the computer program to automatically convert the

Table 5 Best-fit equations for curves in *Figures 12a* and *12b*

η value	Mean $E_h^{NR'}/E_h^{NR}$	Mean plus standard deviation $E_h^{NR'}/E_h^{NR}$
0.4	$E_h^{NR'}/E_h^{NR} = 1.29e^{-1.36T}$ (12)	$E_h^{NR'}/E_h^{NR} = 1.37e^{-1.07T}$ (5.2)
0.6	$E_h^{NR'}/E_h^{NR} = 1.16e^{-2.17T}$ (14)	$E_h^{NR'}/E_h^{NR} = 1.35e^{-1.84T}$ (15)
0.8	$E_h^{NR'}/E_h^{NR} = 1.99e^{-0.57T}$ (16)	$E_h^{NR'}/E_h^{NR} = 1.41e^{-1.74T}$ (17)
1.0	$E_h^{NR'}/E_h^{NR} = 2.23e^{-0.84T}$ (18)	$E_h^{NR'}/E_h^{NR} = 2.67e^{-5.04T}$ (19)
1.2	$E_h^{NR'}/E_h^{NR} = 1.81e^{-0.75T}$ (20)	$E_h^{NR'}/E_h^{NR} = 2.12e^{-5.93T}$ (21)
1.4	$E_h^{NR'}/E_h^{NR} = 1.36e^{-0.46T}$ (22)	$E_h^{NR'}/E_h^{NR} = 1.35e^{-6.66T}$ (23)

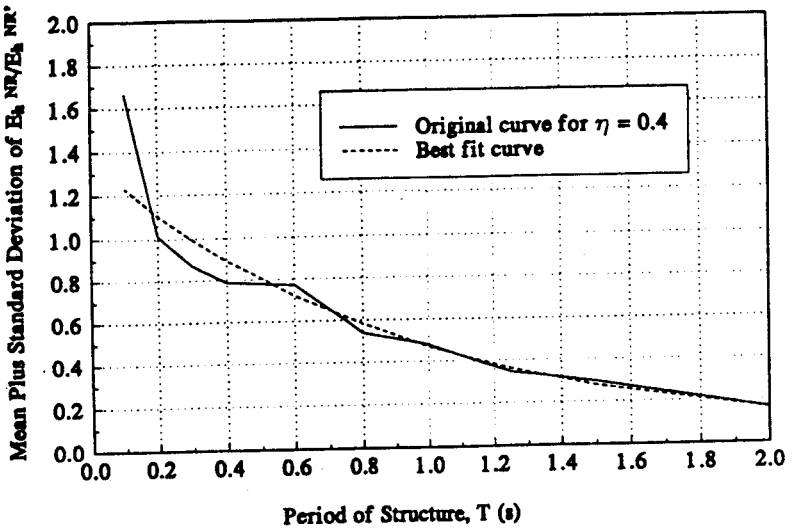

Figure 13 Example of best fit to original data for mean ratiospectra and $\eta = 0.4$

earthquake into equivalent rectangular pulses, the predicted normalized hysteretic energy obtained is 16.55. This value is only a preliminary predicted value of $E_h^{NR'}$ and needs to be revised to obtain the final result. According to *Figure 12*, the mean ratio of $E_h^{NR'}$ to E_h^{NR} is about 0.487, while the mean plus one standard deviation value from either *Figure 12b* or equation (15) is 0.647. Thus, for a one standard deviation of uncertainty, the true predicted normalized hysteretic energy demand of such a structure varies between 25.58 (16.55 over 0.647) and 50.61 (16.55 over 0.327), with an average value of 33.98 (16.55 over 0.487). To obtain the predicted non-normalized hysteretic energy itself, the normalized value needs to be multiplied by the structural yielding strength and displacement. Assuming the mass of the SDOF system in this example to be 1000 kg, its yield strength is then

$$R_y = \eta \times M\ddot{u}_{gmax} = 0.6 \times 1000 \times 3.417 = 2050.2 \text{ (N)} \tag{9}$$

since the maximum ground acceleration, $\ddot{u}_{gmax}$, is 3.417 m/s for this earthquake. The corresponding yield displacement is

$$\Delta_y = \frac{R_y}{K} = \frac{R_y}{\left(\frac{2\pi}{T}\right)^2 M} = \frac{2050.2}{\left(\frac{2\pi}{0.4}\right)^2 \times 1000}$$

$$\doteq 8.32 \times 10^{-3} \text{ (m)} \tag{10}$$

Thus, the predicted hysteretic energy demand for this SDOF system is

$$E_h' = E_h^{NR'} (R_y \Delta_y) \doteq 580 \text{ (J)} \tag{11}$$

where $E_h^{NR'}$ is taken as its mean value, i.e. 33.98.

This predicted value of E_h' can be easily checked using the NONSPEC computer program for this same SDOF system and the El Centro earthquake. The resulting exact hysteretic energy demand calculated is 555.4 J, an error of only about 4.4%.

This example illustrates that the concept and procedure of the equivalent rectangular pulses method is quite promising for predicting the hysteretic energy demand of a SDOF system. Eventually, more earthquake records, instead of just the five earthquakes considered in this research, should be taken into account to make the ratio spectra more reliable. Moreover, earthquakes with frequency characteristics specific to certain geographic regions, as suggested by many researchers[8,10–12], could be considered to further improve the prediction of normalized hysteretic energy.

5.3. Prediction of seismic hysteretic energy using sine-wave excitation spectra

Real earthquakes could also be modelled as a sequence of equivalent sine pulses. The procedure is identical to that previously described with the difference that two adjacent zero crossing points on the time axis of an earthquake ground motion record define a sine pulse of the same maximum acceleration and duration as the actual irregular pulse from the earthquake record. Information on the previously constructed normalized hysteretic energy spectra for sine wave excitation must also be used instead, interpreting each sine pulse as a half-cycle duration sine wave on that spectra. A partial mean ratio spectra of $E_h^{NR'}$ to E_h^{NR} constructed over a limited range of β for the same five earthquakes revealed trends similar to the ratio spectra obtained for the rectangular pulse simulation[9].

Finally, attempts have also been made to predict seismic hysteretic energy spectra by trying to relate the Fourier spectra of an actual earthquake to the previously derived normalized spectra for sine wave excitation. Conceptually, an earthquake acceleration record can be perceived as a large number of simultaneously applied sine or cosine waves having different fundamental periods. The Fourier spectra of the input excitation can be obtained by fast Fourier transform. Unfortunately, as might be expected, individual harmonics alone cannot induce inelastic response due to their small amplitudes, particularly since the amplitude of a continuous Fourier spectra is a function of the number of digitization points. Although it was attempted to remedy this shortcoming by lumping values (areas) over a certain range of fundamental periods, ΔT, for many practical values of ΔT considered, the amplitudes of the resulting pulses were still not sufficiently intense to produce any inelastic response. Hence, attempts to use the Fourier spectra along the lines developed in this paper have so far, been inconclusive.

6. Conclusions

In this paper, normalized energy spectra have been constructed for SDOF systems subjected to rectangular pulse and sine-wave ground excitations, using two approaches to energy normalization. A methodology has also been formulated to predict the hysteretic energy demands of elastoperfectly plastic SDOF systems subjected to real earthquakes based on the availability of normalized spectra for simpler excitations. Some important conclusions of this research project are summarized below.

The selected energy normalization methods, one using maximum ground velocity square and structural mass as a normalization basis, the other structural yield strength and displacement, both produce useful dimensionless energy values; they are also very easily determined for simple rectangular pulse and sine wave excitations.

Normalized predicted hysteretic energy can easily be obtained for actual earthquakes excitations by: firstly, converting these earthquakes into equivalent pulses; secondly, summing the values read for each pulse from the normalized hysteretic energy spectra constructed for simple rectangular pulse or sine wave excitations; and finally, adjusting the total values by ratio spectra or equations statistically calibrated against a number of real earthquake records. The procedure is simple, rapid, and allows direct and reliable prediction of hysteretic energies without the need to resort to complex and time consuming step-by-step nonlinear inelastic time-history analyses.

Future research on this topic is needed to extend the applicability of the findings and to improve the fundamental understanding of the behaviour of the respective energy terms during earthquake excitations. In particular, such research should include: firstly, a study of the frequency content of the earthquakes anticipated in various regions of the world, to determine the range of the normalized hysteretic spectra for pulse and sine wave excitations necessary for use in the above prediction method. Secondly, consideration of other force–displacement structural models, i.e. structural systems having hysteretic behaviour more complex than the bilinear elastoperfectly plastic model used herein. Thirdly, construction of more reliable or geographically dependent ratio spectra by the consideration of more earthquake records. And finally, development of energy-based seismic design methods for the evaluation and design of seismic resistance of existing and new structures.

Acknowledgments

Financial assistance provided by the Natural Sciences and Engineering Research Council of Canada is gratefully acknowledged. The findings and recommendations in this paper, however, are those of the writers and not necessarily those of the sponsor.

References

1 Uang, C. M. and Bertero, V. V. 'Use of energy as a design criterion in earthquake-resistant design', Report UCB/EERC-88/18, Earthquake Engineering Research Centre, University of California, Berkeley, CA, 1988
2 Bruneau, M. and Wang, N. 'Some aspects of energy methods for the inelastic response of ductile SDOF structures', *Engng Struct.* 1996, **18** (1), 1–12
3 Léger, P. and Dussault, S. 'Seismic energy dissipation in MDOF structures', *J. Struct. Engng, ASCE*, 1992, **118** (5), 853–858
4 Fajfar, P., Vidic, T. and Fischinger, M. 'A measure of earthquake motion capacity to damage medium-period structures', *Soil Dyn. Earthquake Engng* 1991, **9**, 236–242
5 Mahin, S. A. and Lin, J. 'Construction of inelastic response spectra for single-degree-of-freedom systems', Report UCB/EERC-83/17, Earthquake Engineering Centre, University of California, Berkeley, CA, 1983
6 Biggs, J. M. *Introduction to structural dynamics* McGraw-Hill, New York, 1964
7 Conte, J. P., Pister, K. S. and Mahin, S. A. 'Influence of the earthquake ground motion process and structural properties on response characteristics of simple structures', Report UCB/EERC-90/09, Earthquake Engineering Centre, University of California, Berkeley, CA, 1990
8 Clough, R. W. and Penzien, J. *Dynamics of structures* McGraw-Hill, New York, 1975
9 Wang, N. 'Normalized energy-based methods to predict the seismic ductile energy response of single-degree-of-freedom structures', M.A.Sc. thesis, University of Ottawa, Canada, 1994
10 Housner, G. W. and Jennings, P. C. 'Generation of artificial earthquakes', *J. Engng Mech. Div., ASCE* 1974, **100** (EM1), 113–150
11 Bertero, V. V. and Mahin, S. A. 'Establishment of design earthquakes-evaluation of present methods', *Int. Symp. Earthquake Struct. Engng*, 1976
12 Chopra, A. K. and Lopez, O. A. 'Evaluation of simulated ground motions for predicting elastic response of long period structures and inelastic response of structures', *Earthquake Engng. Struct. Dyn.* 1979, **7** (4), 383–402